



Electrochemical deposition of platinum on fluorine-doped tin oxide: The nucleation mechanisms

Young-Seon Ko^a, Young-Uk Kwon^{a,b,*}

^a Department of Chemistry, BK-21 School of Chemical Materials Science, Sungkyunkwan University, 300 Chunchun Dong, Jang-An Gu, Suwon 440-746, Republic of Korea

^b SKKU Advanced Institute of Nanotechnology, Sungkyunkwan University, Suwon 440-746, Republic of Korea

ARTICLE INFO

Article history:

Received 12 May 2010

Received in revised form 28 June 2010

Accepted 3 July 2010

Available online 30 July 2010

Keywords:

Electrochemical deposition

Platinum

Fluorine-doped tin oxide

Nucleation mechanism

Mass-transfer-controlled

ABSTRACT

We report the electrochemical formation of Pt particles on fluorine-doped tin oxide electrodes by varying the concentration of PtCl_4^{2-} ions and the overpotentials within the mass-transfer-limited region. The nucleation mechanisms are considered based on the results obtained by cyclic voltammetry, chronoamperometry, and scanning electron microscopy; the nucleation mechanism changes from progressive to instantaneous as the overpotential and the concentration increase. The physical properties of deposited Pt particles, such as particle density, size, and morphology, are also studied with the changes in overpotential, concentration of PtCl_4^{2-} ions, or both.

© 2010 Elsevier Ltd. All rights reserved.

1. Introduction

A dye-sensitized solar cell (DSSC) is typically composed of a dye-modified oxide electrode, a Pt counter electrode, and an electrolyte containing a redox couple. In most of the work on DSSCs, the Pt electrodes have been fabricated by either the thermal decomposition of Pt reagents or sputtering [1–3]. Recently, a number of groups have applied the electrochemical methods in the fabrication of Pt electrodes [4–7]. This approach appears to have some advantages over the other conventional ones in that it can easily prepare Pt electrodes with high-quality at low-costs. Furthermore, the electrochemical methods do not require high temperature, which makes it possible to fabricate flexible Pt electrodes, leading to the future development of wearable electronics. Indeed, these points have been well addressed in the early papers [4–7]. Yoon et al. prepared the electrodeposited Pt electrodes with large surface area using the plating solution containing octaethylene glycol monohexadecyl ether as a structure-directing surfactant [4]. Kim et al. reported the pulse current electrodeposition to fabricate the flexible Pt electrodes with controlled size of nanoparticles and good electrocatalytic activity [6]. However, the detailed understanding on the deposition mechanism of Pt on fluorine-doped tin oxide (FTO) or indium tin oxide electrodes is still lacking.

Generally, electrochemical deposition of a metal is much more complicated on the surface of a semiconductor than on that of a metal because charge carriers in the conduction band, the valence band, or both participate in the deposition process. In almost all of the cases, electrochemical deposition of metals on foreign substrates, especially semiconductor electrodes, follows the Volmer–Weber mechanism [8–10]. Because of the three-dimensional nature of this nucleation and growth mechanism, the surface area regarding a catalytic reaction of deposited Pt particles depends on their physical properties such as particle density, size, and morphology. Accordingly, not only understanding the nucleation and growth mechanism during the deposition process but also controlling those physical properties with the overpotential or the concentration is one of the most important issues in this field.

In this paper, we performed a comprehensive investigation on the electrochemical deposition process of Pt particles on FTO electrodes. The effects of overpotentials or concentrations on the nucleation and growth mechanisms and particle density, size, and morphology have been considered to gain deeper insights.

2. Experimental

Pt was electrochemically deposited on a FTO glass (Pilkington, $8 \Omega/\text{square}$) from a solution containing x mM of potassium tetrachloroplatinate ($x = 5, 10, \text{ and } 20$, Aldrich, 98%) and 0.5 M sulfuric acid (Aldrich, 99.999%) in distilled water (Milli-Q, $\rho > 18 \text{ M}\Omega/\text{cm}$). The plating solution was purged with N_2 for 10 min before the experiments. The FTO glass was sonicated in acetone and, then,

* Corresponding author at: Department of Chemistry, BK-21 School of Chemical Materials Science, Sungkyunkwan University, 300 Chunchun Dong, Jang-An Gu, Suwon 440-746, Republic of Korea. Tel.: +82 31 290 7070; fax: +82 31 290 7075.

E-mail address: ywkwon@skku.edu (Y.-U. Kwon).

in distilled water, and heated at 300 °C or 400 °C for 10 min to clean the surface. All electrochemical experiments were performed in a three-electrode cell at room temperature. A working electrode was prepared by wrapping a part of the clean FTO glass with an insulating tape to make a fixed geometric area of ca. 0.45 cm². A Ag/AgCl electrode was employed as the reference electrode, and a Pt wire was employed as the counter electrode.

Prior to the electrochemical deposition of Pt, a potential of 0.70 V was applied for 5 s to suppress the onset of the Pt deposition. Subsequently, a potential of –0.050 V, –0.10 V, –0.15 V, or –0.20 V was applied to deposit Pt, and a potential of 0.70 V was again applied for 5 s to prohibit additional deposition of Pt that may occur when the potential is slowly decreased. All of the applied potentials used in this experiment were controlled by a potentiostat (Ivium Compactstat).

Field emission scanning electron microscopy (FE-SEM; JEOL JSM-6700F and JSM-7401F) in the backscattered electrons (BSE) mode was used to determine the particle density and to measure the size of Pt particles on the substrate. Between 200 and 1500 particles were counted from each sample to obtain accurate statistical data.

3. Results and discussion

3.1. Cyclic voltammetry

Fig. 1 shows cyclic voltammograms in the potential range of –0.30 V to 1.0 V at FTO electrodes of a 0.5 M H₂SO₄ solution (curve a) and of a 0.5 M H₂SO₄ and 5 mM K₂PtCl₄ solution (curve b). The shape of curve b is nearly similar to those reported in the literature [11]. The current increases from 0.14 V due to the deposition of Pt and decreases from 0.010 V because PtCl₄^{2–} ions are depleted in the vicinity of the electrode surface. The potential range with the depletion corresponds to the mass-transfer-limited region. Below –0.070 V, the current increases and a second peak appears at around –0.14 V. This peak is caused by the adsorption of hydrogen ions on the deposited Pt. At more negative potentials than –0.20 V, the current increases sharply due to the hydrogen evolution. On reversing the scan direction to an anodic sweep from –0.30 V, three peaks emerge due to the oxidation of hydrogen gas and the desorption of hydrogen ions. Stripping of Pt does not occur. The cathodic current is maintained up to 0.50 V, indicating that the presence of Pt on the electrode greatly reduces the overpotential for the deposition of Pt.

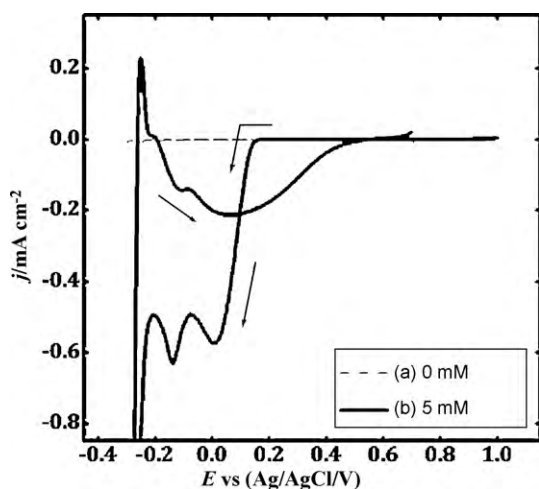


Fig. 1. Cyclic voltammograms at FTO electrodes of a 0.5 M H₂SO₄ solution (broken line, a) and a solution containing 0.5 M H₂SO₄ and 5 mM K₂PtCl₄ (solid line, b). The scan rate was 10 mV/s.

3.2. Nucleation and growth of platinum

3.2.1. Current–time transients

In order to analyze the nucleation and growth processes of electrochemical deposition, either of the two mechanisms, charge-transfer-controlled and mass-transfer-controlled, has to be suppressed. A sufficiently negative potential can make the deposition process mass-transfer-controlled by making the surface concentration of electroactive species very small [12,13]. In this study, therefore, we employed potentials of –0.050 V, –0.10 V, –0.15 V, and –0.20 V within the mass-transfer-limited region based on the curve b in Fig. 1. These potentials are more positive than the potentials at which the hydrogen evolution is dominant. Current–time transient at each of the applied potentials was obtained from plating solutions of three different concentrations, as shown in Fig. 2A–C. The trend in these transients indicates that the Pt deposition follows the three-dimensional nucleation mechanism with mass-transfer-controlled growth [14–17]. The maximum current (J_{max}) and the time at which J_{max} appears (t_{max}) change as a function of the applied potential and the molar concentration of the plating solution.

3.2.2. Analyses of current–time transients

We analyzed the current–time transients using the mathematical model that Scharifker and Hills have derived (hereafter, SH theory). The SH theory describes the three-dimensional nucleation process based on the current–time transients. The nucleation process is explained with two major mechanisms, instantaneous and progressive. The instantaneous nucleation refers to the mechanism in which all the nuclei form instantaneously at the beginning and grow at the same rate. The progressive nucleation involves new nuclei that consecutively form during the whole deposition process [14,15]. According to the SH theory, the mathematical expressions in a non-dimensional form are given by

$$\frac{J^2}{J_{max}^2} = \frac{1.9542}{t/t_{max}} (1 - e^{-1.2564(t/t_{max})})^2 \quad (1)$$

for instantaneous nucleation, and

$$\frac{J^2}{J_{max}^2} = \frac{1.2254}{t/t_{max}} (1 - e^{-2.3367(t/t_{max})})^2 \quad (2)$$

for progressive nucleation [14,15].

Fig. 2D–F shows the $(J/J_{max})^2$ versus t/t_{max} plots of our experimental data. The curves due to Eq. (1) are depicted as dashed lines and the ones due to Eq. (2) as solid lines. When PtCl₄^{2–} concentration is low ($[PtCl_4^{2-}] = 5$ mM), all of the experimental data at the four different potentials are located between the progressive and instantaneous nucleation mechanisms. On the contrary, when PtCl₄^{2–} concentration is higher ($[PtCl_4^{2-}] = 10$ and 20 mM), the mechanism changes from the close-to-progressive nucleation to the instantaneous nucleation as the applied potential gets more negative.

Although some experimental data are deviated from the theoretical lines at longer times ($t/t_{max} > 1$), these deviations are often reported in the literature [17,18]. Radisic et al. demonstrated that the hydrogen evolution could induce such deviations [17]. We believe that the adsorption of hydrogen ions can also cause deviations during the Pt deposition process with large overpotentials. However, the reasons for the deviations from the SH theory have not yet been elucidated thoroughly [18].

3.2.3. Analyses of SEM images

In order to verify our electrochemical data, we followed the changes of the particle density during the deposition processes under various conditions. For this purpose, we obtained SEM images of the FTO electrodes with Pt deposited under various

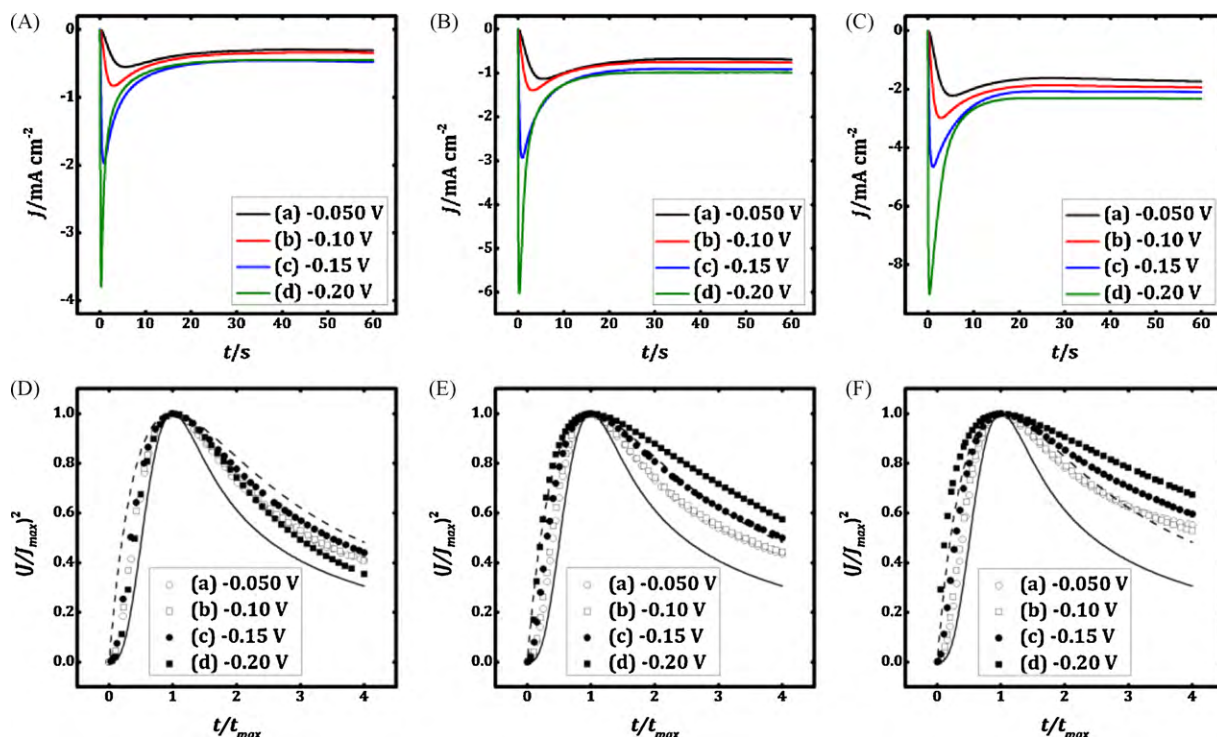


Fig. 2. (A–C) Potentiostatic current–time transients on FTO electrodes at various potentials in the range from -0.050 V to -0.20 V and (D–F) dimensionless plots for the normalized experimental current–time transients. Plating solutions of three different concentrations of electrodepositing species were used: (A and D) 5 mM K_2PtCl_4 ; (B and E) 10 mM K_2PtCl_4 ; (C and F) 20 mM K_2PtCl_4 . In (D–F), the dashed lines refer to instantaneous nucleation and solid lines refer to progressive nucleation.

deposition conditions. The images were obtained in the BSE mode, by which the contrast between Pt and FTO could be significantly enhanced, enabling precise counting of the Pt particles. Fig. 3 shows some of the representative SEM images.

In Fig. 4A, we delineate the changes in the particle density with deposition time under several different conditions. When the potential of -0.20 V is imposed to 10 mM and 20 mM K_2PtCl_4 solutions (cases b and d, respectively), the particle densities are held constant throughout the whole deposition processes, which are consistent with the instantaneous nucleation mechanism. However, for the potential of -0.050 V in the 10 mM K_2PtCl_4 solution (case a) and the potential of -0.20 V in the 5 mM K_2PtCl_4 solution (case c), the particle densities initially increase and then are held constant with the deposition time, implying the progressive nucleation mechanism.

The changes in particle sizes and the corresponding standard deviations depending on the deposition condition (Fig. 4B) also provide information on the nucleation mechanisms. For all cases, regardless of the deposition conditions, the particle size and the corresponding standard deviation increase with the increase of deposition time. The increase in particle size arises from the amount of charge passed during the deposition process. The irregular distribution of particles causes an inhomogeneous flux of $PtCl_4^{2-}$ ions within the overlapped diffusion zone and therefore the particle size distribution is bound to broaden for any nucleation mechanisms [19–21]. Nevertheless, the extent of the particle size distribution differs between the two nucleation mechanisms. In particular, the particle size distribution before the overlap of the diffusion zones around the particles represents the character of each mechanism because each particle is not affected by the inhomogeneous flux of electrodepositing species.

The relative standard deviation (RSD) of the particle diameter is calculated to represent the particle size distribution. At t/t_{max} smaller than unity, the cases of a, b, c, and d in Fig. 4B have the RSDs of 41.5%, 25.5%, 26.8%, and 22.8%, respectively. Due to the for-

mation of new nuclei during the deposition process, the progressive nucleation is expected to have a larger RSD than the instantaneous nucleation. Thus, the nucleation mechanism of the case a is identified to be progressive and those of cases b and d instantaneous, consistent with the results from the analyses of the particle densities. Though the case c has a small RSD, it can be identified as progressive nucleation because its small RSD is a consequence of the low-concentration of $PtCl_4^{2-}$ ions. In Fig. 4A, the saturated particle density decreases as the concentration of the plating solution becomes low. The low nuclear density means that the average distance between particles is long and the flux of electrodepositing species becomes more uniform around most of the particles [19–21]. Accordingly, the particle size distribution can be narrow at the initial step ($t/t_{max} \leq 1$) under low-concentration-conditions despite the progressive nucleation.

Therefore, we can conclude that the SEM data agree with the electrochemical data in Fig. 2 in differentiating the two nucleation mechanisms. Both sets of data indicate that the nucleation mechanism is changed from progressive to instantaneous as the overpotential and concentration increase simultaneously.

3.3. The influence of overpotentials beyond the deposition time of t_{max}

For the purpose of preparing Pt films in most of the applications, it is customary to deposit for longer times than t_{max} . In this section, we explored the effects of overpotential on such Pt films. We employed SEM to analyze the trend of particle density and size with overpotentials (or applied potentials). Pt was deposited for over 1.2 – $3.6t_{max}$ for all the samples. These extents of deposition are sufficient for the saturated particle density to be estimated because the particle density approaches 95% of its saturation value at t_{max} for the progressive nucleation [9,14]. Fig. 5A shows that the particle density initially increases with overpotential and then remains constant from the applied potential of -0.15 V for all concentra-

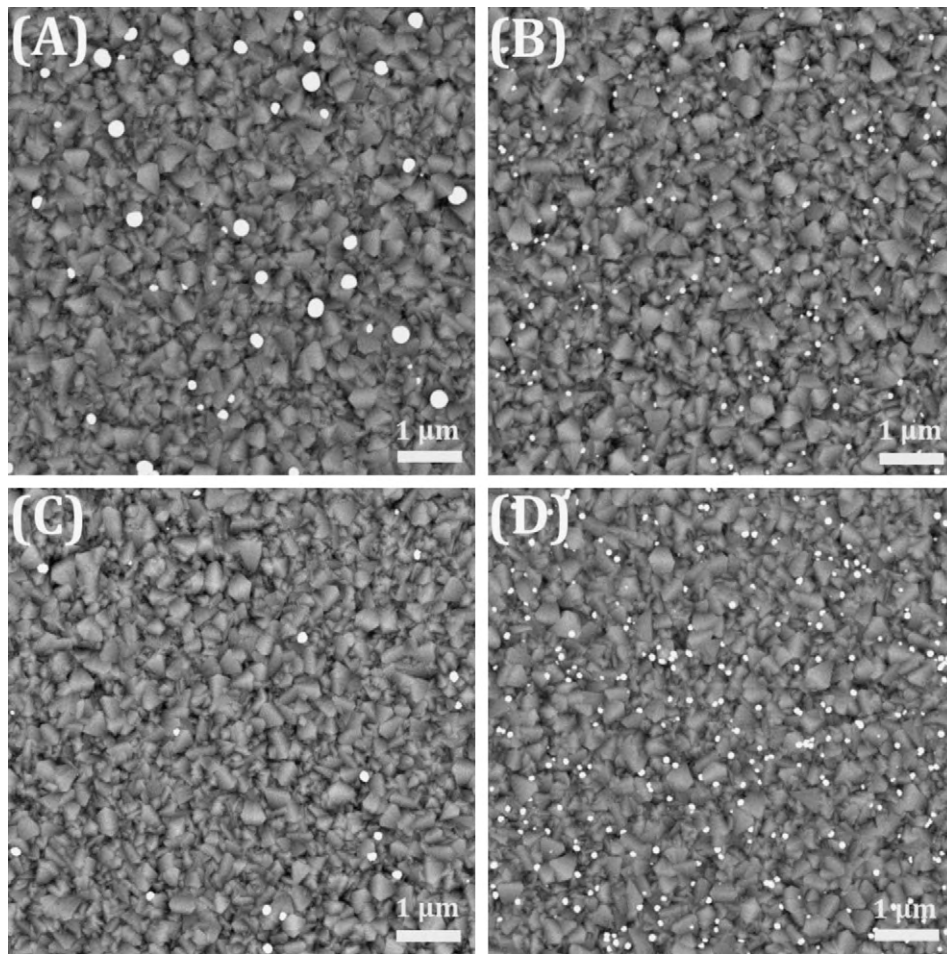


Fig. 3. SEM images of Pt particles deposited on the surface of FTO electrode for $t = t_{max}$ under different conditions: (A) 10 mM, -0.050 V; (B) 10 mM, -0.20 V; (C) 5 mM, -0.20 V and (D) 20 mM, -0.20 V.

tions of PtCl_4^{2-} ions. For the electrochemical deposition of metals on foreign substrates, the nucleation sites have different activation energies for nucleation [22,23]. The unchanged particle densities in the potential range of -0.15 V to -0.20 V are probably attributed to saturation of the number of nucleation sites because these overpotentials are sufficiently large to activate almost all of the nucleation sites on the electrode surface.

On the other hand, the particle size decreases as the overpotential increases (the applied potential becomes more negative), as

shown in Fig. 5B. The decreased particle sizes are closely associated with the increase in particle densities when the overpotential is high. During the deposition process, the flux of PtCl_4^{2-} ions approaches the diffusion zones surrounding the Pt particles. And the neighboring diffusion zones are overlapped with one another. Because there are a few particles within the overlapped diffusion zones, the total flux of PtCl_4^{2-} ions is also divided into a few fluxes toward each particle. For this reason, the flux density of PtCl_4^{2-} ions is much weaker on each particle within overlapped diffusion zones

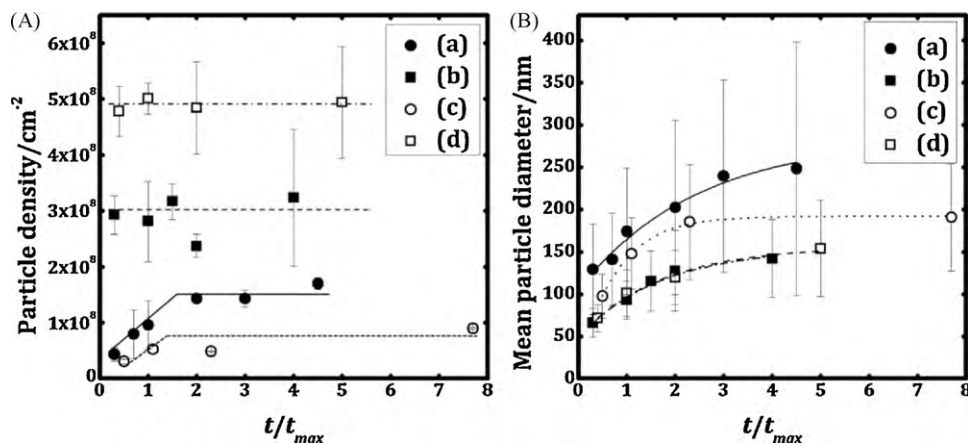


Fig. 4. (A) Particle density and (B) mean diameter of Pt particles as a function of the normalized deposition time, t/t_{max} , under various conditions. The lines in (A) are guidelines and the lines in (B) are the exponential fits to the data points. (a) 10 mM, -0.050 V; (b) 10 mM, -0.20 V; (c) 5 mM, -0.20 V and (d) 20 mM, -0.20 V.

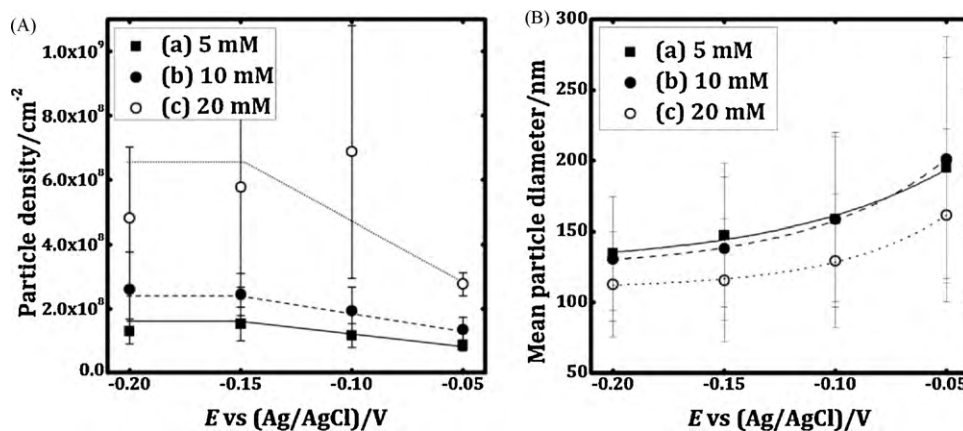


Fig. 5. (A) Particle density and (B) mean diameter of Pt particles as a function of the applied potentials at different concentrations of PtCl_4^{2-} ions. The lines in (A) are guidelines and the lines in (B) are the exponential fits to the data points.

than on a particle within a single diffusion zone not overlapped. In summary, when the overpotential increases, the particle density increases and, concurrently, the diffusion zones are more overlapped with one another. Therefore, the particle sizes are decreased due to the decline in flux density of PtCl_4^{2-} ions.

Fig. 6 shows SEM images of electrodeposited Pt particles depending on overpotentials in the 20 mM K_2PtCl_4 solution. At the applied potential of -0.050 V (low overpotential), the morphology of Pt particles seems to be a hemispherical shape with the smooth

surface. On moving from low overpotentials to high overpotentials, the surface of Pt particles becomes rougher, which probably results in increasing the surface area. At low-concentrations of PtCl_4^{2-} ions (5 mM and 10 mM K_2PtCl_4 solution), likewise, the same phenomena were observed in morphology; the surface of Pt particles becomes rougher with increasing the overpotential. However, the morphology of their surface is hardly changed when the concentration is varied only under the constant overpotential (not shown here). To obtain the quantitative results of the surface area, we performed the

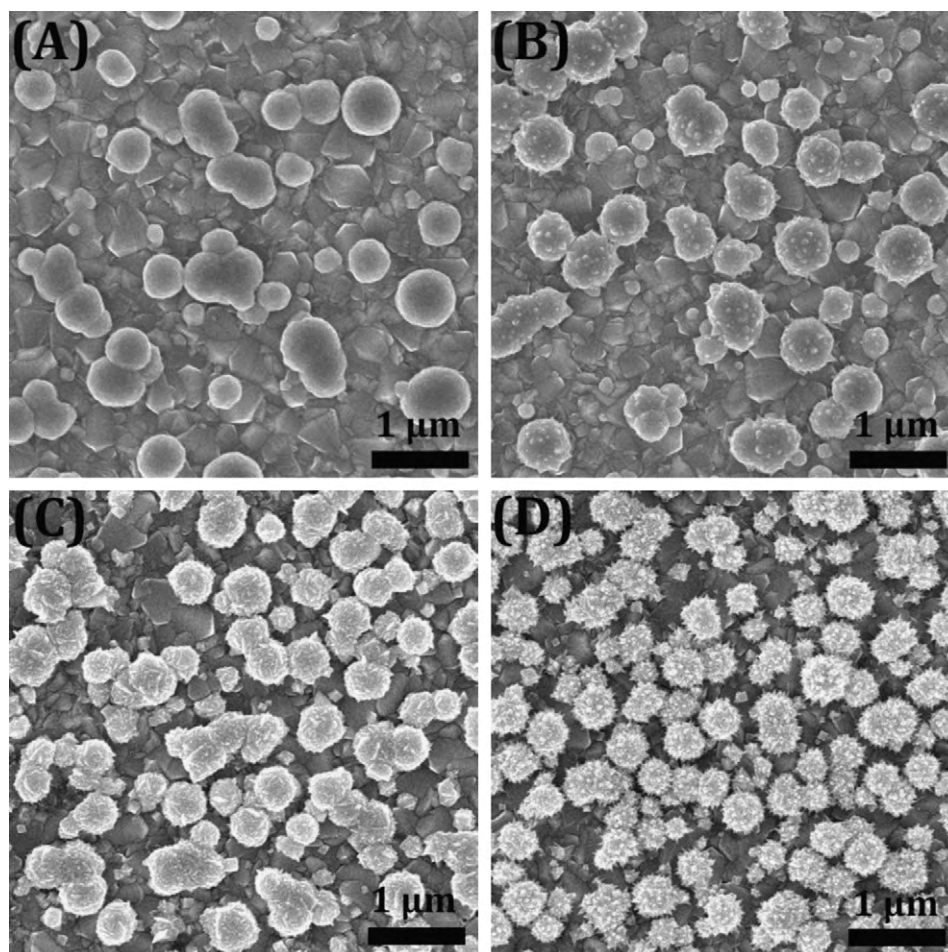


Fig. 6. SEM images of Pt particles deposited on the surface of FTO electrode for 60 s at the identical concentration of PtCl_4^{2-} ions (20 mM K_2PtCl_4 solution) but different applied potentials: (A) -0.050 V; (B) -0.10 V; (C) -0.15 V and (D) -0.20 V.

Table 1Particle density (N), size, surface area, and morphology of electrochemically deposited Pt for 60 s from a 10 mM K_2PtCl_4 solution under different applied potentials.

	Applied potential vs. (Ag/AgCl)/V			
	−0.050	−0.10	−0.15	−0.20
$N (\times 10^8 \text{ cm}^{-2})^a$	1.3 ± 0.4	1.9 ± 0.7	2.4 ± 0.7	2.6 ± 0.1
Particle size (nm) ^a	201 ± 87	158 ± 62	138 ± 51	131 ± 44
Surface area ($\text{m}^2 \text{ cm}^{-2}$) ^b	0.59 ± 0.08	0.72 ± 0.1	1.1 ± 0.1	1.1 ± 0.05
Morphology ^a	The surface of Pt particles gets rougher on moving left to right			

^a The particle density, size, and morphology were determined by the observations of SEM images.^b The surface area of Pt particles was calculated by the integration of the hydrogen ions-desorbed region on cyclic voltammograms.

cyclic voltammetry of electrodeposited Pt particles in 0.5 M H_2SO_4 aqueous solution. The scan rate was 0.1 V/s. The electrochemical data including the surface area as well as the particle density, size, and morphology are summarized in Table 1. As the overpotential increases, the surface area also increases due to the increased particle density and the rougher surface. However, the surface areas at the applied potentials of −0.15 V and −0.20 V are the same with each other. This phenomenon can be explained by the fact that the particle density is saturated and the particle size gets smaller when the overpotential is high although the surface of Pt particles seems to be rougher at −0.20 V than at −0.15 V.

4. Conclusions

We investigated the nucleation and growth mechanisms of electrochemical deposition process of Pt particles on the FTO electrode by varying the concentration of $PtCl_4^{2-}$ ions and the overpotentials within the mass-transfer-limited region. Based on the results obtained by analyses of SEM images and current–time transients with the SH theory, the nucleation mechanism changes from progressive to instantaneous as the overpotential and concentration increase. The increase in these two parameters also enhances the particle density. In particular, the morphology of the particle surface becomes rougher when the overpotential increases rather than the concentration does. Thus, the surface area of the platinized electrode increases although its surface area remains constant at the high overpotentials probably due to the saturation of the particle density and the decline in the particle size. Because a catalytic reaction occurs on the surface of particles, the efficiency of the reaction is dependent on the surface area. Consequently, both of the overpotential and the concentration are the important parameters to easily control those properties that affect the catalytic activity. In this regard, our experimental results are expected to provide useful information, such as controlling the particle density, size, and morphology with the overpotential or the concentration, on electrochemical deposition of Pt on the FTO electrode.

Acknowledgements

This work was supported by grants NRF-20090094024 (Priority Research Center Program), NRF-2010-0015035 (Basic Science Research Program NCRC), and KETEP 2009-3021010030-11-1 (Research Center of Break-through Program CIGS). We thank CCRF for the SEM data.

References

- [1] N. Papageorgiou, W.F. Maier, M. Grätzel, *J. Electrochem. Soc.* 144 (1997) 876.
- [2] Y.-S. Ko, M.-H. Kim, Y.-U. Kwon, *Bull. Korean Chem. Soc.* 29 (2008) 463.
- [3] X. Fang, T. Ma, G. Guan, M. Akiyama, T. Kida, E. Abe, *J. Electroanal. Chem.* 570 (2004) 257.
- [4] C.H. Yoon, R. Vittal, J. Lee, W.-S. Chae, K.-J. Kim, *Electrochim. Acta* 53 (2008) 2890.
- [5] P. Li, J. Wu, J. Lin, M. Huang, Z. Lan, Q. Li, *Electrochim. Acta* 53 (2008) 4161.
- [6] S.-S. Kim, Y.-C. Nah, Y.-Y. Noh, J. Jo, D.-Y. Kim, *Electrochim. Acta* 51 (2006) 3814.
- [7] G. Tsekouras, A.J. Mozer, G.G. Wallace, *J. Electrochem. Soc.* 155 (2008) K124.
- [8] E. Budevski, G. Staikov, W.J. Lorenz, *Electrochemical Phase Formation and Growth: An Introduction to the Initial Stages of Metal Deposition*, VCH, Weinheim, 1996.
- [9] L. Guo, A. Radisic, P.C. Searson, *J. Phys. Chem. B* 109 (2005) 24008.
- [10] R.M. Stiger, S. Gorer, B. Craft, R.M. Penner, *Langmuir* 15 (1999) 790.
- [11] G. Lu, G. Zangari, *J. Phys. Chem. B* 109 (2005) 7998.
- [12] M.E. Hyde, R.G. Compton, *J. Electroanal. Chem.* 549 (2003) 1.
- [13] A.J. Bard, L.R. Faulkner, *Electrochemical Methods: Fundamentals and Applications*, 2nd ed., John Wiley & Sons, Inc., New York, 2001.
- [14] B. Scharifker, G. Hills, *Electrochim. Acta* 28 (1983) 879.
- [15] G. Gunawardena, G. Hills, I. Montenegro, B. Scharifker, *J. Electroanal. Chem.* 138 (1982) 225.
- [16] F. Gloaguen, J.M. Léger, C. Lamy, A. Marmann, U. Stimming, R. Vogel, *Electrochim. Acta* 44 (1998) 1805.
- [17] A. Radisic, J.G. Long, P.M. Hoffmann, P.C. Searson, *J. Electrochem. Soc.* 148 (2001) C41.
- [18] D. Grujicic, B. Pesic, *Electrochim. Acta* 47 (2002) 2901.
- [19] J.L. Fransaer, R.M. Penner, *J. Phys. Chem. B* 103 (1999) 7643.
- [20] H. Liu, R.M. Penner, *J. Phys. Chem. B* 104 (2000) 9131.
- [21] R.M. Penner, *J. Phys. Chem. B* 106 (2002) 3339.
- [22] G. Oskam, P.M. Vereecken, P.C. Searson, *J. Electrochem. Soc.* 146 (1999) 1436.
- [23] G. Oskam, P.C. Searson, *J. Electrochem. Soc.* 147 (2000) 2199.